OPTIMIZATION OF A STORAGE RING PRE-INJECTOR FOR HIGH TRANSMISSION EFFICIENCY AND LOW ENERGY SPREAD*

W. Xu[1], F. Zhang[1], Z. Dong[1], Z. Shao[2], T. Zhang[†2], L. Wang[‡1,2], Y. Lu[1,2]
[1]University of Science and Technology of China, Hefei, China
[2]Hefei National Laboratory, Hefei, China

Abstract

In this paper, the Non-dominated Sorting Genetic Algorithm II (NSGA-II), combined with the beam dynamics code ASTRA, was employed for the multi-objective optimization of the output performance of an electron linear accelerator (linac). Taking the pre-injector of a storage ring light source as an example, the electron linac consists of a thermionic cathode high-voltage electron gun, a sub-harmonic buncher (SHB), a buncher, and a traveling-wave accelerator tube. Maximizing the transmission efficiency and minimizing the rms energy spread were defined as the core objectives of the optimization. The optimization results indicate that the beam energy at the linac exit reaches approximately 65 MeV, with the transmission efficiency exceeding 70 % and the rms energy spread maintained below 0.35 %.

INTRODUCTION

Linacs are widely used in medical treatment, industry and scientific research. In the scientific research field, serving as an injector/pre-injector for storage ring light sources, free-electron lasers (FELs) and colliders, electron linacs provide electron beams to generate high-quality light sources, supporting cutting-edge research in physics, chemistry, biology, materials science and medicine [1].

For storage ring light sources, electron linacs are most commonly used as pre-injectors. In this role, the pre-injector forms the low-energy front end of the accelerator chain and conditions the beam emerging from the electron gun by performing longitudinal phase-space manipulation, bunch compression, and initial acceleration. These processes establish the beam parameters required for efficient booster capture, making transmission efficiency and energy spread key optimization objectives. Efficient pre-injector performance is particularly important for compact storage ring facilities, where the available accelerating length and construction cost are often constrained.

The pre-injector configuration used in this work is shown in Fig. 1. It includes a high-voltage thermionic cathode electron gun, a six-harmonic sub-harmonic buncher (SHB), a buncher, and a traveling-wave accelerating structure. Multiple solenoids placed in the low-energy region suppress space-charge-induced emittance growth, allowing high-quality beam formation within a compact layout. This work targets compact and cost-effective storage ring pre-injectors capable of achieving high transmission efficiency and low rms energy spread with a limited number of accelerating structures.

Given the strong space-charge effects and nonlinear RF dynamics involved, numerical optimization is widely used in pre-injector design, with MOGA and MOPSO being common approaches [2–6]. In this study, NSGA-II [7] was used to optimize the RF phases and solenoid magnetic fields for high transmission efficiency and low rms energy spread. The RF voltages were subsequently adjusted to maintain the target beam energy during the optimization process. The optimization procedure and resulting beam performance are presented in the following sections.

BEAM DYNAMICS SIMULATION

Start-to-End Simulation Setup

To evaluate the beam dynamics performance of the proposed pre-injector scheme, start-to-end simulations were carried out using the ASTRA code [8]. An initial simulation with 1×10^4 macro-particles was performed to establish a reasonable working point. The number of macro-particles was then increased to 5×10^4 to improve statistical accuracy and numerical stability. Further increase of the macro-particle number produced no significant change in the optimized beam parameters, indicating satisfactory numerical convergence.

Electrons are emitted from a high-voltage thermionic cathode electron gun. The initial particle distribution was generated using the CST Particle Tracking solver and assumed to be uniform in both the transverse and temporal directions. The electron gun operates in the space-charge-limited regime, and the Space Charge emission model implemented in CST was employed in the simulations. The main beam parameters at the gun exit are summarized in Table 1. Four solenoid magnets are placed in the low-energy section to mitigate strong space-charge effects and suppress emittance growth, ensuring proper beam transport and focusing.

Table 1: Beam Parameters at the Electron Gun Exit

Parameter	Value
Energy [keV]	100
Charge [nC]	1
Full bunch length [ns]	1
RMS beam size σ_x/σ_y [mm]	2.683 / 2.685

The electron beam sequentially passes through a 0.499654 GHz standing-wave sub-harmonic buncher (SHB),

* Work supported by the National Natural Science Foundation of China (No. 12405173) and the Anhui Provincial Natural Science Foundation (No. 2508085QA013, Youth Project, Category C)
† zhangtong@hfnl.cn
‡ wanglin@ustc.edu.cn

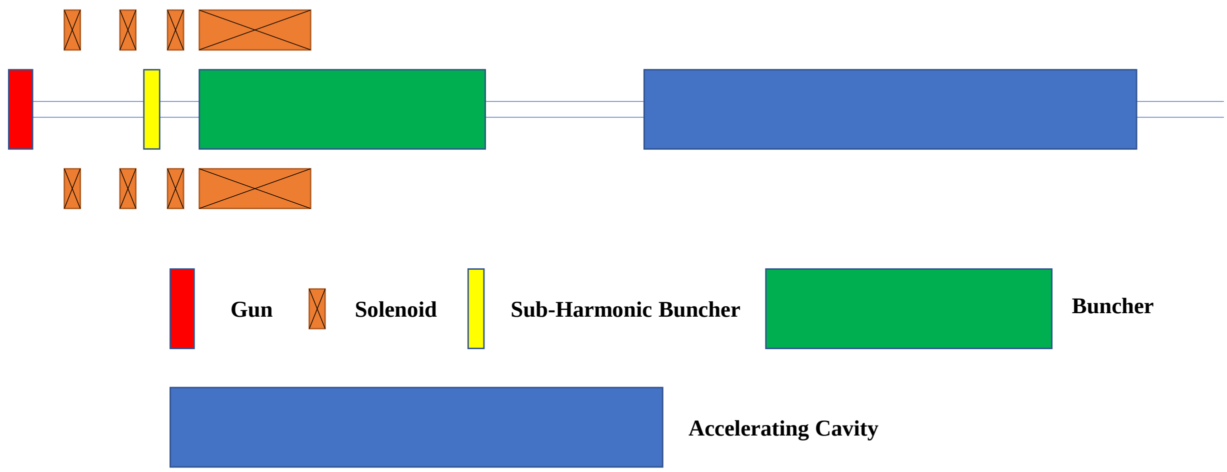

Figure 1: The layout of the pre-injector.

an S-band buncher, and a main accelerating structure operating at 2.997924 GHz. The buncher is a $2\pi/3$ traveling-wave structure composed of six phase-velocity-tapered cells and forty-eight constant-velocity cells (54 cells in total). The main accelerating structure is a 2.997924 GHz S-band $2\pi/3$ traveling-wave cavity with 90 cells, accelerating the beam to approximately 65 MeV.

In the initial simulation stage, key operating parameters were manually tuned based on physical intuition to establish a stable working point. Subsequently, the NSGA-II was employed to perform multi-objective global optimization based on the Pareto optimality principle. The optimization aims to maximize the transmission efficiency and minimize the rms energy spread, with solenoid magnetic fields, SHB phase, buncher phase, and accelerating cavity phase selected as optimization variables. The parameter ranges were determined according to the manually optimized results (Table 2). A population size of 200 and 50 generations were used. Parallel computation was employed, with eight optimization jobs executed simultaneously.

Table 2: Beam Dynamics Optimization Parameters

Parameter	Manual Setting	Optimization Range
Solenoid Peak Magnetic Fields (T)		
Solenoid 1	0.012	0–0.02
Solenoid 2	0.010	0–0.02
Solenoid 3	0.010	0–0.02
Solenoid 4	0.065	0–0.10
RF Cavity Phases (deg)		
Sub-buncher	95	90–100
Buncher	50	45–55
AC cavity	5	−5–5

Simulation Results and Analysis

Figure 2 presents the Pareto front obtained from the multi-objective optimization. NSGA-II gradually approaches the non-dominated solution set in the multidimensional parameter space, yielding a compromise between transmission efficiency and rms energy spread. In this work, a solution with a rms energy spread of approximately 0.34 % and a transmission efficiency of about 73 % is chosen as the operating point.

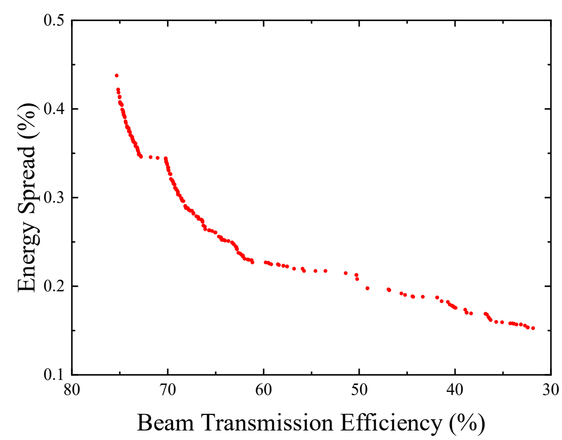

Figure 2: Pareto front.

Figure 3 shows the evolution of beam parameters along the beamline after optimization. The transverse rms beam size and normalized rms emittance increase in the low-energy region due to strong space-charge effects and are effectively controlled by solenoid focusing. As the beam energy increases, space-charge effects become less significant, resulting in stable transverse beam parameters in the high-energy section. The rms energy spread is reduced through longitudinal compression and off-crest acceleration, eventually stabilizing below 0.35 %.

Figures 4 and 5 illustrate the longitudinal phase-space distributions at the buncher exit and the pre-injector exit, respectively, before and after optimization. In both stages, the optimized beam exhibits a significantly more compact distribution, indicating effective suppression of the rms energy spread and improved longitudinal beam quality. A clear phase-space rotation is observed from the buncher exit to the pre-injector exit, where the longitudinal correlation evolves from negative to positive. This behavior originates from

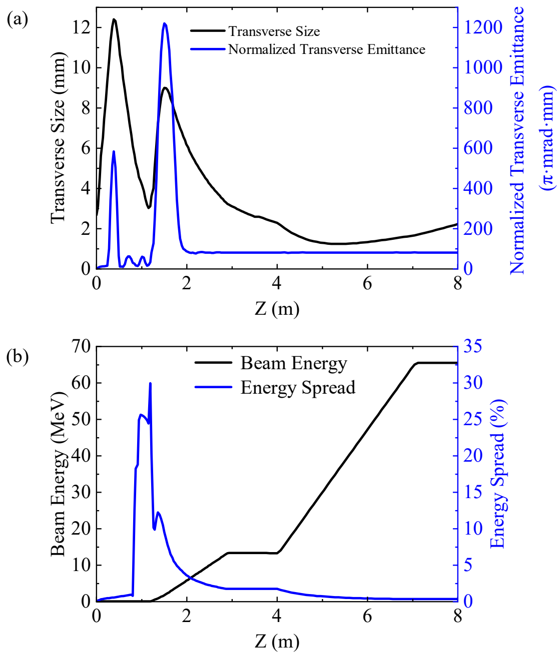

Figure 3: Beam parameter evolution after optimization, showing (a) transverse rms size and normalized rms emittance and (b) mean energy and rms energy spread along the beamline.

the velocity modulation introduced by the buncher and the subsequent off-crest acceleration in the main cavity, which compensates the initial energy chirp and minimizes the final projected rms energy spread.

In summary, the optimization results validate the effectiveness of the proposed pre-injector design. The final beam energy reaches approximately 65 MeV, with a transmission efficiency exceeding 70 % and a rms energy spread below 0.35 %, meeting the injection requirements of the storage ring light source.

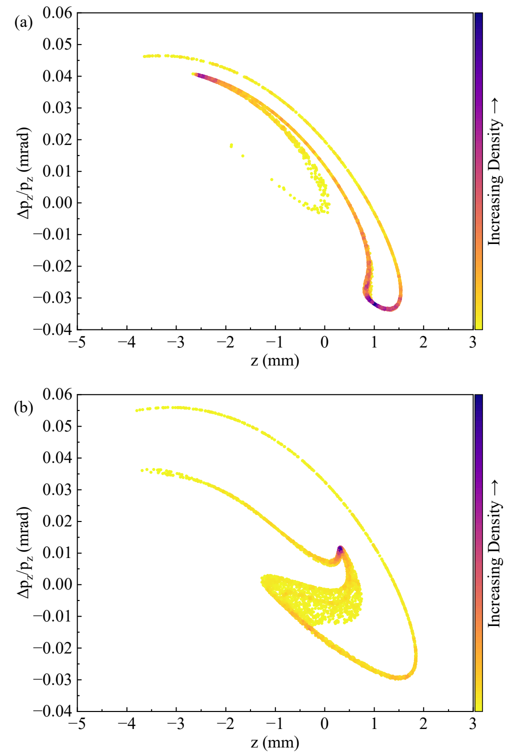

Figure 4: Longitudinal beam distributions at the buncher exit with (a) manual parameter tuning and (b) NSGA-II optimization.

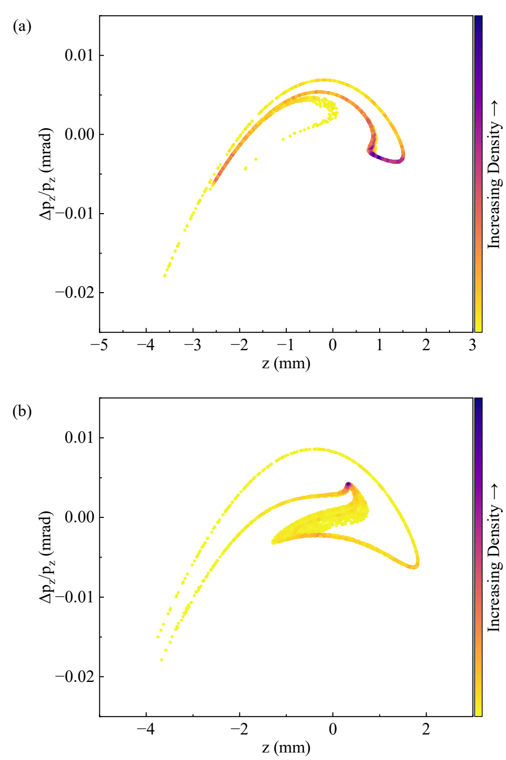

Figure 5: Longitudinal beam distributions at the pre-injector exit with (a) manual parameter tuning and (b) NSGA-II optimization.

CONCLUSION

In this work, a multi-objective optimization framework based on NSGA-II, combined with ASTRA start-to-end simulations, was applied to the design of a storage ring pre-injector. The solenoid fields, SHB phase, buncher phase, and accelerating-cavity phase were jointly optimized to achieve high transmission efficiency and low rms energy spread.

The optimized configuration increases the beam energy to approximately 65 MeV and achieves a transmission efficiency above 70 % while maintaining the rms energy spread below 0.35 %. Beam dynamics analyses further confirm effective suppression of transverse emittance growth and improved longitudinal beam quality.

These results demonstrate that the proposed optimization strategy is effective for improving pre-injector performance and can be extended in future work to include additional optimization variables and beamline parameters.

REFERENCES

[1] X. Zhang, *Synchrotron Radiation Applications*. Singapore: World Scientific, 2018. doi:10.1142/10643

[2] C. Kim, E.-S. Kim, S. H. Park, C. S. Park, C.-K. Min, and W. J. Byeon, "Error analysis study for electron linear accelerator optimized using multi-objective genetic algorithm", *J. Korean Phys. Soc*, vol. 86, no. 1, pp. 23–30, 2025. doi:10.1007/s40042-024-01232-2

[3] L. Liu *et al.*, "Simulation study of high-quality electron beam injector for external injection of laser plasma wakefield acceleration", *Nucl. Eng. Technol.*, vol. 57, no. 7, p. 103531, 2025. doi:10.1016/j.net.2025.103531

[4] C. Gulliford, A. Bartnik, I. Bazarov, and J. Maxson, "Multiobjective optimization design of an rf gun based electron diffraction beam line", *Phys. Rev. Accel. Beams*, vol. 20, no. 3, p. 033401, 2017. doi:10.1103/PhysRevAccelBeams.20.033401

[5] R. Bartolini, M. Apollonio, and I. Martin, "Multiobjective genetic algorithm optimization of the beam dynamics in linac drivers for free electron lasers", *Phys. Rev. Spec. Top. Accel. Beams*, vol. 15, no. 3, p. 030701, 2012. doi:10.1103/PhysRevSTAB.15.030701

[6] L. Yang, D. Robin, F. Sannibale, C. Steier, and W. Wan, "Global optimization of an accelerator lattice using multiobjective genetic algorithms", *Nucl. Instrum. Methods Phys. Res. A*, vol. 609, no. 1, pp. 50–57, 2009. doi:10.1016/j.nima.2009.08.027

[7] K. Deb, A. Pratap, S. Agarwal, and T. Meyarivan, "A fast and elitist multiobjective genetic algorithm: nsga-ii", *IEEE Trans. Evol. Comput.*, vol. 6, no. 2, pp. 182–197, 2002. doi:10.1109/4235.996017

[8] *ASTRA: A Space Charge Tracking Algorithm*, DESY, Hamburg, Germany, 2017. http://www.desy.de/~mpyflo/